Synlett C. W. Tornøe et al. Cluster

# Divergent Protein Synthesis of Bowman–Birk Protease Inhibitors, their Hydrodynamic Behavior and Co-crystallization with α-Chymotrypsin

**Christian W. Tornøe** *[a]
**Eva Johansson**[b]
**Per-Olof Wahlund**[c]

[a] Department of Protein & Peptide Chemistry, Novo Nordisk, Novo Nordisk Park, 2760 Måløv, Denmark
cwet@novonordisk.com
[b] Department of Protein & Peptide Structure, Novo Nordisk, Novo Nordisk Park, 2760 Måløv, Denmark
[c] Department of Large Protein Biophysics, Novo Nordisk, Novo Nordisk Park, 2760 Måløv, Denmark

Published as part of the Cluster *Recent Advances in Protein and Peptide Synthesis*

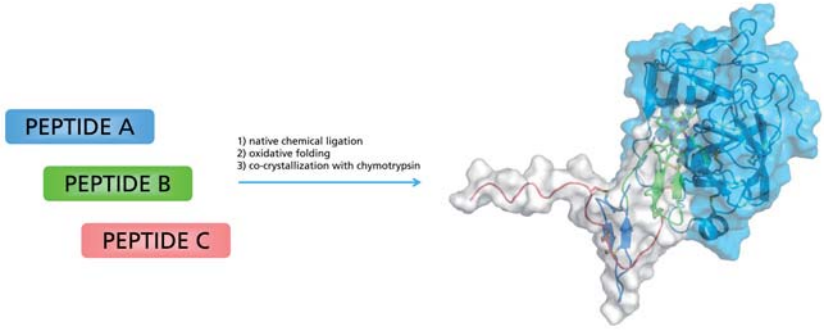


Received: 28.03.2017
Accepted after revision: 30.04.2017
Published online: 24.05.2017
DOI: 10.1055/s-0036-1588840; Art ID: st-2017-w0211-c

**Abstract** A divergent protein synthesis strategy was executed to effectively synthesize Bowman–Birk protease inhibitor (BBI) analogues using native chemical ligation of peptide hydrazides. Grafting selected residues from a potent trypsin inhibitor, sunflower trypsin inhibitor-1, onto the α-chymotrypsin-binding loop of BBI, resulted in a fourfold improvement of α-chymotrypsin inhibition. The crystal structure of a synthetic BBI analogue co-crystallized with α-chymotrypsin confirmed the correct protein fold and showed a similar overall structure to unmodified BBI in complex with α-chymotrypsin. Dynamic light scattering showed that *C*-terminal truncation of BBI led to increased self-association.

**Key words** protein synthesis, divergent synthesis, Bowman–Birk protease inhibitor, X-ray crystallography, α-chymotrypsin, native chemical ligation

Many cellular processes are regulated by protein–protein interactions (PPIs), which are attractive targets for disease modulation, either by improving or destabilizing PPIs.[1] Optimization of small-molecule drug leads often relies on minor molecular changes by iteratively addition or removal of substituents or manipulating heteroatoms in aromatic rings. This approach has been used with success in transforming small-molecule[2] and peptide[3] leads into clinical candidates, but protein leads are more challenging to optimize due to their larger size and increased complexity.[4] Grafting peptide or protein epitopes onto cyclic peptides, such as sunflower trypsin inhibitor-1 or cyclotides, a family of macrocyclic peptides with three disulfide bridges known as a cystine knot, has been used to simplify the protein optimization challenge.[5] Instead of synthesizing or expressing the whole protein of interest, analogues of cyclotides (28- to 37-mer peptides), which display the desired protein epitope in a peptide loop region, can be made and tested for effect in blocking or enhancing PPIs.

Protease inhibitors have the potential to regulate various diseases, and HIV treatment is a prime example of peptide-derived protease inhibitors that have been successful in the clinic.[6] Selectivity of small-molecule protease inhibitors against related proteases can be difficult to achieve, and thus larger molecules, for example, protein-based, may be required to obtain the desired selectivity, due to the larger surface area of interations.[7] High-throughput generation of molecular diversity in a protein format is necessary to effectively optimize PPIs, for example, inhibition of proteases, and this requires a good expression system and protein purification or efficient chemical synthesis of proteins. Besides improving the interaction between protein and protease, it is also important to investigate macroscopic properties of the drug candidate, such as chemical and physical stability in solution.

Bowman–Birk Inhibitor protein (BBI) is a cysteine-rich miniprotein (71 amino acids) found in seeds,[8] where it helps protect against insects and pathogens through its function as a protease inhibitor.[9] The protein is rich in cysteine residues, which comprise 20% of all amino acids in BBI, resulting in a densely cross-linked protein structure, that display high stability towards elevated temperature and acidic treatment.[10] Two hairpin loops, each consisting of a disulfide-linked nine-residue loop (Scheme 1), project from the BBI core, and can inhibit trypsin and α-chymotrypsin independently or simultaneously, in a ternary complex.[11] BBI is often extracted from soybeans, and it has been tested in clinical trials where it was considered nontoxic and well tolerated (patients received 2–3 g BBI daily).[12] BBI has also been described as a natural functional food ingredient, as there is approx. 100 mg BBI in 1 L of soya milk.[13]

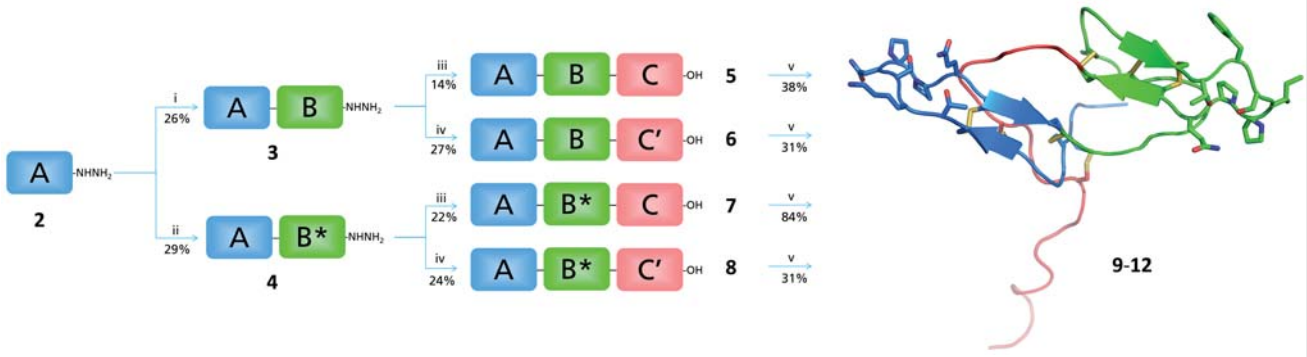


**Scheme 1** Bowman–Birk Inhibitor analogues prepared by native chemical ligation using $NaNO_2$/MESNa activation of peptide hydrazides. i) BBI(24-50,27L)-$NHNH_2$ (**16** = B), ii) BBI(24-50,27L,42T,43F,45I,47P)-$NHNH_2$ (**17** = B*), iii) BBI(51-71)-OH (**18** = C), iv) BBI(51-65)-OH (**19** = C′), v) oxidative folding at pH 7.9. * denotes mutations, ′ denotes truncation.

Earlier protein chemistry work on BBI by Odani and Ono[14] enabled single amino acid substitution in P1 of carboxyl-protected BBI demonstrating that α-chymotrypsin inhibition was retained when Met, Phe, or Trp replaced Leu43.

The carboxyl-protected BBI analogues were prepared by α-chymotrypsin-mediated cleavage of the Leu43-Ser44 bond, excision of Leu43 by carboxypeptidase A, and carbodiimide coupling of an amino acid methyl ester. Leatherbarrow et al. simplified the BBI protein into a bicyclic 16-mer, by merging the two hairpin loops into one cyclic structure, where the hairpin disulfide bridge was shared between the two loops,[15] but no chemical synthesis of BBI has previously been reported.

The aim of this research was to utilize the BBI scaffold and synthesize analogues using native chemical ligation in a diversity generating manner, fold the cysteine-rich proteins and improve α-chymotrypsin inhibition. Amino acid substitutions from the very potent trypsin inhibitor sunflower trypsin inhibitor-1 (SFTI-1) were used to make a BBI/SFTI-1 chimera combined with substitution of Leu in P1 to Phe. The X-ray structure of a synthetic BBI analogue co-crystallized with α-chymotrypsin was used to confirm the correct protein fold and was compared to the BBI:α-chymotrypsin complex crystal structure. Furthermore, dynamic light scattering of full-length and truncated BBI was used to investigate differences in their self-association.

Synthesis of BBI peptide segments was done at room temperature using SPPS with DIC/Oxyma Pure® activation of amino acids on a Prelude® synthesizer. Trifluoroacetic acid mediated cleavage and protecting group removal followed by purification using RP-HPLC afforded the five protein segments (**2**, **16**, **17**, **18**, and **19**, also named A, B, B*, C, and C′ in Scheme 1) in 8–40% yield and high purity. The freeze-dried peptides were used to synthesize the full-length proteins (Scheme 1) by exploiting the latent thioester properties of the C-terminal hydrazides.[16] By assembling the proteins in a divergent manner (Scheme 1) using native chemical ligation of peptides,[17] the number of reaction steps needed to generate the four BBI analogues was lower compared to a linear strategy. Activation of the N-terminal segment **2** with sodium nitrite ($NaNO_2$) and sodium 2-mercaptoethanesulfonate (MESNa) afforded a thioester, which was split in two and reacted with segment **16** and segment **17**, to afford **3** and **4**.[18] Compound **3** and **4** were then activated by $NaNO_2$/MESNa and split in two, so each compound could react with the C-terminal segments **18** and **19**. As a consequence of the chosen mutations (vide infra) being located in the middle and C-terminal segments of BBI, a divergent synthesis strategy was utilized to efficiently generate analogues **5**–**8** in a total of six ligation steps from five segments (illustrated in Scheme 1). If each protein was synthesized in two steps without using common intermediates (e.g., **3** and **4**), a total of eight ligation steps would be needed. The final oxidative folding was performed at high dilution (0.05 mg/mL) to minimize misfolding and protein aggregation.[19] Protein folding of the linear analogues was successful, even in the presence of mutations in the α-chymotrypsin binding loop and/or C-terminal truncation. The folded proteins only required buffer exchange and ultrafiltration to concentrate the folded proteins (**9**–**12**), as they were pure enough for testing in vitro without further purification.[20] Chemiluminescence nitrogen detection[21] was used to determine the exact protein concentrations, and the folding yields of the final proteins ranged from 31–84%.

Bowman–Birk inhibitor (BBI, **1**) from soybeans, the synthetic Bowman–Birk inhibitor analogues (**9**–**12**), SFTI-1 (**13**), and [Phe5]-SFTI-1 (**14**), were all synthesized and evaluated for their trypsin and α-chymotrypsin inhibition. This was done by using fluorogenic substrates and measuring the increase in fluorescence upon addition of either trypsin or α-chymotrypsin and reported in Table 1.

**Table 1** Inhibition of α-Chymotrypsin and Trypsin

| | Compound | Chymotrypsin $EC_{50}$ (nM) | Trypsin $EC_{50}$ (nM) |
|---|---|---|---|
| **1** | BBI (from soybeans) | 59 | 25 |
| **9** | 27L-BBI | 130 | 20 |
| **10** | 27L,des(66-71)-BBI | 150 | 50 |
| **11** | 27L,42T,43F,45I,47P-BBI | 16 | 32 |
| **12** | 27L,42T,43F,45I,47P,des(66-71)-BBI | 80 | 60 |
| **13** | cyclo-(GR*C*TKSIPP*I*CFPD) (SFTI-1) | >1000 | 26 |
| **14** | cyclo-(GR*C*TFSIPP*I*CFPD) ([Phe5]-SFTI-1) | 46 | 103 |

'*C*XXXXXXX*C*' denotes a disulfide bond between the two cysteines. 'Cyclo-' denotes backbone cyclization.

In all four synthetic protein analogues, Met27 (located on the surface of the protein) was replaced with Leu27 to avoid oxidation. No mutations were made in the trypsin binding loop, which is reflected in the in vitro data (Table 1), where all BBI analogues show similar inhibition of trypsin and are comparable with SFTI-1 (**13**).

To optimize the α-chymotrypsin binding loop of BBI (**1**), residues from SFTI-1 (**13**) and knowledge of α-chymotrypsin's substrate specificity were combined and grafted onto BBI to create a BBI/SFTI-1 chimera (**11**). Specifically, Leu43 in P1 was mutated to Phe, because aromatic amino acids (Phe, Tyr, and Trp) are the best substituents in P1 for inhibiting α-chymotrypsin.[22] Furthermore, the small and potent trypsin inhibitor, SFTI-1 (**13**), have a nine amino acid hairpin loop motif, where the substrate specificity could be changed from trypsin to α-chymotrypsin by replacing Lys in P1 with Phe, as reported by the Łęgowska group.[23] The resulting [Phe5]-SFTI-1 (**14**) was a potent α-chymotrypsin inhibitor, but surprisingly, it also retained some trypsin inhibitory activity (103 nM vs. 26 nM for SFTI-1, Table 1), which has not been reported before. This may be explained by the deep S1 pocket in trypsin accommodating Lys when bound to SFTI-1.[24] It is suggested that there may be room for Phe in the S1 pocket, though it cannot form any hydrogen bond to the S1 residue in trypsin, Ser190. The amino acid sequence and bicyclic structure of SFTI-1 has been evolved to exquisitely match the active site of trypsin, resulting in a small, yet potent inhibitor. Ligand efficiency is defined as the binding energy per nonhydrogen atom of the ligand,[25] meaning that smaller ligands (e.g., SFTI-1, 14 residues) are more efficient than larger ligands (e.g., BBI, 71 residues), if they have similar binding energies (e.g., inhibition of trypsin). Monocyclic SFTI-1 (lacking backbone cyclization) is approximately 20-fold less potent when compared to natural, bicyclic SFTI-1 (**13**),[26] but the isolated monocyclic α-chymotrypsin hairpin loop from BBI, Ac-*CALSYPAQC*-$NH_2$ does not inhibit α-chymotrypsin at all.[27] Thus BBI (**1**) must rely on its tertiary structure and flanking amino acids around the hairpin loop (residues 41–49), to obtain potent inhibition of α-chymotrypsin. The apparent suboptimal α-chymotrypsin binding loop in BBI and the higher ligand efficiency of SFTI-1 was the background for grafting four amino acids from [Phe5]-SFTI-1 (**14**) into analogues **11** and **12**. C-Terminal truncation of BBI was also included in the divergent protein synthesis strategy to investigate self-association of analogues without the acidic C-terminal residues (EDDKEN).

A slight decrease in α-chymotrypsin inhibition was observed when Met27 in BBI (**1**) was mutated to Leu27 in **9** (59 nM vs. 130 nM), but when mutations inspired by [Phe5]-SFTI-1 were introduced in the α-chymotrypsin binding loop of BBI, the BBI/SFTI-1 chimera **11** showed a fourfold improvement in α-chymotrypsin inhibition over unmodified BBI (**1**) (16 nM vs. 59 nM). A similar, but smaller effect was also observed in the truncated (des66-71) analogues **10** and **12**, where the latter protein contained the chimeric BBI/SFTI-1 α-chymotrypsin binding loop (150 nM vs. 80 nM).

1.2:1 and 1.5:1 molar mixtures of **11**:α-chymotrypsin or BBI (**1**):α-chymotrypsin, respectively, were screened for crystal growth using hanging drop vapor diffusion, and diffracting crystals were identified. Both complexes, **11**:α-chymotrypsin and BBI (**1**):α-chymotrypsin, crystallized in the same crystal form with one inhibitor:α-chymotrypsin complex in the asymmetric unit ($P2_12_12$ with $a$ = 75 Å, $b$ = 79 Å and $c$ = 48 Å) and the structures were refined to 2.1 Å and 2.3 Å resolution, respectively.

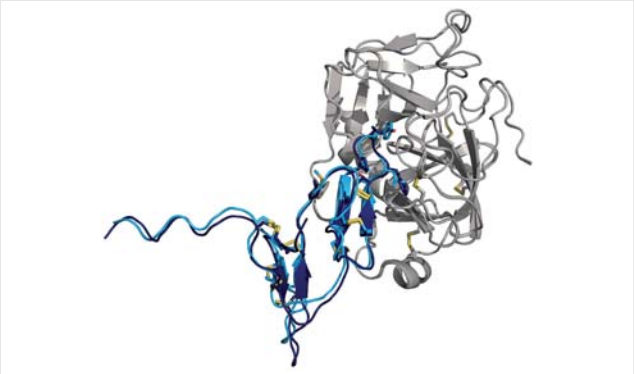

**Figure 1** Cartoon with disulfide bridges in stick representation of superposed co-crystal structures of **1** (cyan) with α-chymotrypsin (light grey) and synthetic **11** (dark blue) with α-chymotrypsin. The side chains of amino acid residues differing between **1** and **11** are shown in stick representation. Both complexes are crystallized in the same crystal form and refined to 2.3Å (**1**:α-chymotrypsin) and 2.1 Å (**11**:α-chymotrypsin) resolution with R/Rfree values of 21.0/26.7% and 19.0/24.1%, respectively.

X-ray crystallography of the binary complex between α-chymotrypsin and BBI (**1**) or the BBI analogue (**11**) showed the same fold and binding of both BBI proteins to α-chymotrypsin (Figure 1).

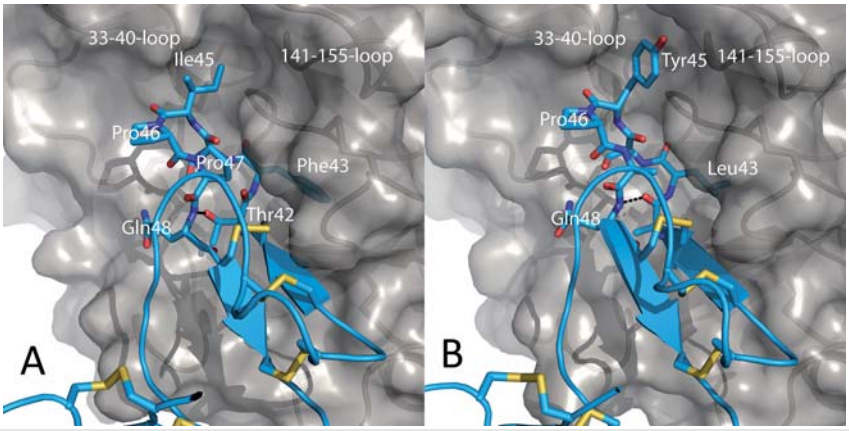


**Figure 2** Zoomed view of the α-chymotrypsin binding pocket (grey) and residues 42–48 (stick form) from **11** (view A) and BBI (**1**, view B), respectively. The hydrogen bonds between the Gln48 backbone amide and the Thr42 hydroxyl group (A) or Ala42 backbone carbonyl (B) are shown as black dotted lines.

In the **11**:α-chymotrypsin complex the entire Phe43 amino acid residue is clearly pulled further into the α-chymotrypsin S1 pocket also resulting in withdrawal of the Thr42 backbone carbonyl group and thereby preventing the hydrogen-bond formation to the Gln48 backbone amino group found in the BBI (**1**):α-chymotrypsin complex (Figure 2, A and B, respectively). The mutation Ala42Thr provides the possibility of an alternative hydrogen-bond formation between the Thr42 hydroxyl group and the amide group from the backbone of Gln48, stabilizing the conformation of the α-chymotrypsin bound **11** in the same manner. The Tyr45Ile mutation does not fill out the space between the 33–40 loop and 141–155 loop of α-chymotrypsin and may leave an exposed hydrophobic surface disrupting the possible stacking interactions of Tyr45. Residues 44–47 of **1** and **11** form a β-turn type IVb and in this type of turn, *i* + 2 is always a *cis*-proline residue (residue 46 in this case). The Tyr45Ile and Ala47Pro modifications stabilize this type of turn with similar preferences for the Tyr/Ile at *i* + 1 and Ala/Pro at *i* + 3. The introduction of the Pro47 residue makes the structure more rigid and facilitates the Thr42 to Gln48 hydrogen bond mentioned above.

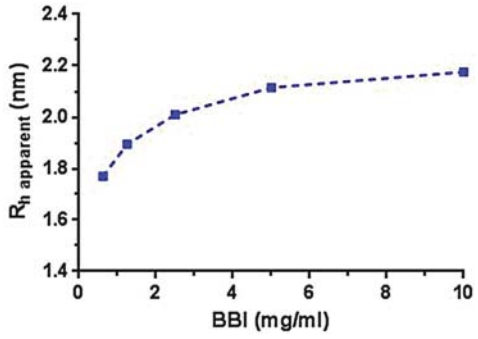


**Figure 3** Hydrodynamic radius of BBI (**1**) in 10 mM Tris buffer, 150 mM NaCl, pH 8.5

Dynamic light-scattering measurements and analysis of self-association for BBI (**1**) in the presence of 150 mM NaCl at pH 8.5 are shown in Figure 3. The obtained data are in agreement with self-association equilibrium between monomer–dimer–trimer as reported in literature.[11b]

The hydrodynamic behavior of two BBI analogues were investigated and compared with BBI (**1**). The three BBI proteins were analyzed by dynamic light scattering at a concentration of 5 mg/mL, and the results are presented in Table 2. BBI (**1**) had no sign of large aggregates and hence cumulant fit was used while regularization had to be used for the synthetic BBI analogues **9** and **10** since both contained 0.5% aggregates with $R_h$ of 25–60 nm. The change from Met to Leu at position 27 of BBI had no significant effect on the apparent $R_h$ implying similar self-association behavior as BBI (**1**) as presented in Table 2. When the last six amino acids of the C-terminal were removed (des66-71) the apparent $R_h$ of **10** increased significantly, compared to BBI (**1**) and **9**. The C-terminal truncation removed three negative charges and hence less charge–charge repulsion on intra- as well as intermolecular level was expected. The larger apparent hydrodynamic size was therefore likely due to stronger self-association.

**Table 2** Hydrodynamic Radii of Three Different BBI Analogues[a]

| | Compound | Calculated charge at pH 8 | Concentration (mg/mL) | Rh (nm) |
|---|---|---|---|---|
| **1** | BBI | –6.8 | 5 | 2.08 ± 0.02 |
| **9** | 27L-BBI | –6.8 | 5 | 2.04 ± 0.04 |
| **10** | 27L,des(66-71)-BBI | –3.8 | 5 | 4.05 ± 0.04 |

[a] Hydrodynamic radii of three different BBI analogues in 10 mM Tris, 100 mM NaCl, pH 8.0. The charge is the theoretical net charge calculated from the amino acid sequence.

Four Bowman–Birk inhibitor analogues were synthesized using peptide hydrazides and native chemical ligation. Using a divergent synthesis strategy, all four proteins were generated efficiently and folded to afford potent inhibitors of trypsin and α-chymotrypsin. The α-chymotrypsin binding loop of BBI (**1**) was mutated to improve α-chymotrypsin inhibition with inspiration from the natural SFTI-1 (**13**) and its analogue [Phe5]-SFTI-1 (**14**). A fourfold improvement of α-chymotrypsin inhibition was obtained (**11**, α-chymotrypsin $EC_{50}$ = 16 nM) and X-ray crystal structural data from the **11**:α-chymotrypsin complex revealed that Phe43 bound deeper in the S1 pocket of α-chymotrypsin compared to Leu43 in BBI (**1**). The mutations in the hairpin loop of **11** allowed for a new stabilizing hydrogen bond between Thr42 to Gln48 but also prevented the original Ala42 to Gln48 hydrogen bond found in BBI (**1**). C-Terminal truncation (des66-71) of the Bowman–Birk analogues **9** and **11** led to a slight decrease in trypsin inhibition and varying loss of α-chymotrypsin inhibition (up to fivefold loss for 27L,42T,43F,45I,47P,des(66-71)-BBI (**12**), when compared to the full-length analogue **11**). The apparent hydrodynamic size of the analogues in solution was measured using dynamic light scattering, and the Leu27 mutation of BBI did not change $R_h$ (**9** vs. **1**). However, the removal of three negative charges overall in **10** by removing residues 66–71 led to an increase in $R_h$ from 2 nm to 4 nm, which could be due to less charge–charge repulsions in the truncated analogue **10**.

The power of divergent protein synthesis combining multiple peptide segments and successful grafting of SFTI-1 residues onto BBI allowed the rapid synthesis of potent Bowman–Birk inhibitor analogues, two new co-crystals of α-chymotrypsin with either BBI (**1**) or 27L,42T,43F,45I,47P-BBI (**11**) and new insights into the solution behavior of C-terminally truncated BBI. It is envisioned that divergent protein synthesis may be used to explore and optimize other protein–protein interactions by generating molecular diversity in a high-throughput fashion.

## Acknowledgment

Franta Hubálek and Gitte Norup are thanked for their help in measuring α-chymotrypsin and trypsin inhibition, Thomas Seigert Harkes for crystallization experiments and Janni Larsen for measuring DLS.

## Supporting Information

Experimental details, compound characterization, enzyme inhibition and DLS measurements. Crystal structure coordinates and structure factors have been deposited in PDB entries 5J4Q (BBI (**1**):α-chymotrypsin) and 5J4S (**11**:α-chymotrypsin).Supporting information for this article is available online at https://doi.org/10.1055/s-0036-1588840.

## References and Notes

(1) Scott, D. E.; Bayly, A. R.; Abell, C.; Skidmore, J. *Nat. Rev. Drug Discov.* **2016**, *15*, 533.
(2) Lindsley, C. W.; Weaver, D.; Bridges, T. M.; Kennedy, J. P. In *Chemical Biology*; John Wiley and Sons **2012**, 65.
(3) Edwards, P. J.; LaPlante, S. R. In *Peptide Drug Discovery and Development*; Wiley-VCH: Weinheim, **2011**, 1.
(4) Miranda, L. P.; Shao, H.; Williams, J.; Chen, S.-Y.; Kong, T.; Garcia, R.; Chinn, Y.; Fraud, N.; O'Dwyer, B.; Ye, J.; Wilken, J.; Low, D. E.; Cagle, E. N.; Carnevali, M.; Lee, A.; Song, D.; Kung, A.; Bradburne, J. A.; Paliard, X.; Kochendoerfer, G. G. *J. Am. Chem. Soc.* **2007**, *129*, 13153.
(5) (a) Qiu, Y.; Taichi, M.; Wei, N.; Yang, H.; Luo, K. Q.; Tam, J. P. *J. Med. Chem.* **2017**, *60*, 504. (b) Qu, H.; Smithies, B. J.; Durek, T.; Craik, D. J. *Aust. J. Chem.* **2017**, *70*, 152.
(6) Leung, D.; Abbenante, G.; Fairlie, D. P. *J. Med. Chem.* **2000**, *43*, 305.
(7) Drag, M.; Salvesen, G. S. *Nat. Rev. Drug Discov.* **2010**, *9*, 690.
(8) (a) Bowman, D. E. *Experimental Biol. Med.* **1946**, *63*, 547. (b) Birk, Y.; Gertler, A.; Khalef, S. *Biochem. J.* **1963**, *87*, 281.
(9) (a) Ryan, C. A. *Annu. Rev. Phytopathol.* **1990**, *28*, 425. (b) Habib, H.; Fazili, K. M. *Biotechnol. Mol. Biol. Rev.* **2007**, *2*, 68.
(10) Birk, Y. *Biochim. Biophys. Acta* **1961**, *54*, 378.
(11) (a) Birk, Y.; Gertler, A.; Khalef, S. *Biochim. Biophys. Acta* **1967**, *147*, 402. (b) Birk, Y. *Int. J. Pept. Protein Res.* **1985**, *25*, 113.
(12) (a) Malkowicz, S. B.; McKenna, W. G.; Vaughn, D. J.; Wan, X. S.; Propert, K. J.; Rockwell, K.; Marks, S. H. F.; Wein, A. J.; Kennedy, A. R. *Prostate* **2001**, *48*, 16. (b) Lin, L. L.; Mick, R.; Ware, J.; Metz, J.; Lustig, R.; Vapiwala, N.; Rengan, R.; Kennedy, A. R. *Oncol. Lett.* **2014**, *7*, 1151.
(13) Hernández-Ledesma, B.; Hsieh, C.-C.; de Lumen, B. O. *Food Chem.* **2009**, *115*, 574.
(14) Odani, S.; Ono, T. *J. Biochem.* **1980**, *88*, 1555.
(15) Jaulent, A. M.; Leatherbarrow, R. J. *Protein Eng., Des. Sel.* **2004**, *17*, 681.
(16) Fang, G.-M.; Li, Y.-M.; Shen, F.; Huang, Y.-C.; Li, J.-B.; Lin, Y.; Cui, H.-K.; Liu, L. *Angew. Chem. Int. Ed.* **2011**, *50*, 7645.
(17) Dawson, P.; Muir, T.; Clark-Lewis, I.; Kent, S. *Science* **1994**, *266*, 776.
(18) Native chemical ligation was achieved by dissolution of peptide hydrazide in a mixture of 90:10 0.2 M $Na_2HPO_4$/6 M Gu·HCl and MeCN (pH adjusted to 3.0) at 0° C and addition of $NaNO_2$ (5 equiv). After 20 min, MESNa (50 equiv) and Cys-peptide (1.1 equiv) were added and pH was adjusted to 7.0. Excess 1,4-dithiothreitol was added after 16 h, and the product was purified by RP-HPLC.
(19) Protein folding was achieved by dissolution of unfolded protein in 6 mM Gu·HCl/2 mM mercaptoethanol/0.2 mM GSSG, 0.1 mM EDTA/80 mM Tris (pH 7.9) at 0.05 mg/mL.
(20) UPLC and LC–MS were used to characterize the folded proteins. UPLC (C18 column, 2.1 mm × 150 mm, 95:5 to 5:95 water/MeCN + 0.1% TFA over 16 min). LC–MS (C18 column, 2.1 mm × 50 mm, 95:5 to 5:95 water/MeCN + 0.1% formic acid over 4 min).
Protein **9**: UPLC: $t_R$ 5.1 min, LC–MS: *m/z* calcd 7840.7; found *m/4*: 1961.0, *m/5*: 1569.0, *m/6*: 1307.5, *m/7*: 1121.0, *m/8*: 981.1.
Protein **10**: UPLC: $t_R$ 4.7 min, LC–MS: *m/z* calcd 7110.0; found *m/4*: 1778.2, *m/5*: 1422.7, *m/6*: 1186.0, *m/7*: 1016.7.
Protein **11**: UPLC: $t_R$ 5.2 min, LC–MS: *m/z* calcd 7880.7; found *m/5*: 1577.1, *m/6*: 1314.4, *m/7*: 1126.7, *m/8*: 985.9.
Protein **12**: UPLC: $t_R$ 5.2 min, LC–MS: *m/z* calcd 7150.0; found *m/4*: 1788.5, *m/5*: 1431.0, *m/6*: 1192.6, *m/7*: 1022.4, *m/8*: 894.5.

(21) (a) Fujinari, E. M.; Courthaudon, L. O. *J. Chromatogr. A* **1992**, *592*, 209. (b) Fujinari, E. M. In *Developments in Food Science*; Wetzel, D.; Charalambous, G., Eds.; Elsevier: Amsterdam, **1998**, 431.
(22) Appel, W. *Clin. Biochem.* **1986**, *19*, 317.
(23) (a) Zabłotna, E.; Jaśkiewicz, A.; Łęgowska, A.; Miecznikowska, H.; Lesner, A.; Rolka, K. *J. Pept. Sci.* **2007**, *13*, 749. (b) Debowski, D.; Łukajtis, R.; Filipowicz, M.; Strzelecka, P.; Wysocka, M.; Łęgowska, A.; Lesner, A.; Rolka, K. *Pept. Sci.* **2013**, *100*, 154.
(24) Luckett, S.; Garcia, R. S.; Barker, J. J.; Konarev, A. V.; Shewry, P. R.; Clarke, A. R.; Brady, R. L. *J. Mol. Biol.* **1999**, *290*, 525.
(25) Hopkins, A. L.; Groom, C. R.; Alex, A. *Drug Discovery Today* **2004**, *9*, 430.
(26) Korsinczky, M. L. J.; Schirra, H. J.; Rosengren, K. J.; West, J.; Condie, B. A.; Otvos, L.; Anderson, M. A.; Craik, D. J. *J. Mol. Biol.* **2001**, *311*, 579.
(27) Ando, S.; Yasutake, A.; Waki, M.; Nishino, N.; Kato, T.; Izumiya, N. *Biochim. Biophys. Acta* **1987**, *916*, 527.